

# Evolution of a Triad Twisted String Actuator for Controlling a Two Degrees of Freedom Joint to Improve Performance and Allow for Active Transmission Adjustment

Damian Crosby, Joaquin Carrasco *Member, IEEE*, William Heath *Member, IEEE*, and Andrew Weightman

**Abstract**—

**Index Terms**—Flexible Robots, Force Control, Tendon/Wire Mechanism, Twisted String Actuator.

## I. INTRODUCTION

### II. IMPROVEMENTS TO ORIGINAL DESIGN

#### A. Increasing AUJ Angle Range

The actuated universal joint angle tracking experiments in [1] only had a range of  $\pm 14.5^\circ$  in a single axis, and  $\pm 6^\circ$  for both axes. This was because one or more twisted string actuator would completely “unwind” near that limit and be unable to lengthen further. This limits the practicality of such a mechanism, for example a multi-segment design would have a very large minimum curvature. Increasing  $f_{\min}$  does increase the angle range marginally by increasing the twisted string actuator motor angle at  $\theta = [0 \ 0]^\top$ ,  $\approx$  for the original design, as shown in figure ?? . However, this has other effects that are further explained in section ?? that may be undesirable for the application.

In order to increase the angle range significantly, the value of  $r$  has to be reduced as shown in figure ?? . This can be done by using smaller motors, or by using the same size or larger motors with offset shafts connected by spur gears. Smaller motors were chosen, Micro Metal Gearmotor (50:1), as they were lighter than the existing motors and the mechanism would be less complex. These motors would have a much lower  $\theta_{\max}$  than the existing motors of only  $\text{rad s}^{-1}$  compared to  $\text{rad s}^{-1}$ , but since the original experiments limited the motor velocity to  $\text{rad s}^{-1}$  to ensure mechanism stability, this is not a concern.

This design change allowed  $r$  to be reduced from 13 mm to 7.25 mm. This reduces the twisted string actuator stroke range for a given actuated universal joint angle range accordingly, which also reduces the twisted string actuator

motor angle accordingly, allowing a greater actuated universal joint angle to be reached before one or more twisted string actuator unwind.

#### B. Improving AUJ Angle Measurement Accuracy

The original design used a Bosch Sensortec BNO080 9 degree of freedom inertial measurement unit [2] to measure the actuated universal joint orientation. Originally it was planned for a pair of these inertial measurement unit to be used, one on the base segment and one on the follower segment, and the orientation of the actuated universal joint to be calculated from the difference between them in any orientation. However, the magnetometer measurements proved to be unreliable inside the laboratory, so only a single inertial measurement unit was used and the base segment was orientated with the gravity vector parallel to the  $z$  axis. This allowed the actuated universal joint orientation to be calculated from only the accelerometer readings, but meant the mechanism could only be controlled when orientated in the vertical axis.

There was also an issue with the inertial measurement unit resolution as shown in figure ?? , which is only only accurate to within  $0^\circ$ . A Savitsky-Golay filter was applied to the results in [1] for data presentation purposes and to more accurately represent the true actuated universal joint angles at that point in time.

In order to allow the mechanism to be controllable for any orientation with respect to gravity, a solution that could directly measure the mechanical angular displacement of the universal joint was needed. Two options were considered, potentiometers and hall effect sensors. A potentiometer would couple a shaft of each universal joint spider axes to a resistive track, changing its resistance depending on actuated universal joint orientation and providing an analog voltage signal to the controller. A hall effect sensor would be similar to the potentiometer solution, but would use a radially bipolar magnet on the end of the shaft with a hall effect sensor beneath it, which would also provide an analog voltage signal or digital data for the axial orientation of the magnet, and therefore the shaft [3]. The potentiometer solution was chosen for easy availability of components and simplicity of control since no programming of the sensor would be

D. Crosby, and A. Weightman are with the Department of Mechanical, Aerospace and Civil Engineering, School of Engineering, Faculty of Science and Engineering, The University of Manchester, Manchester, United Kingdom.

J. Carrasco and W. Heath are with the Department of Electrical and Electronic Engineering, School of Engineering, Faculty of Science and Engineering, The University of Manchester, Manchester, United Kingdom.

required. The potentiometer also has mechanical stops, which make it easier to assure the required actuated universal joint angle range will be able to be measured during assembly. The hall effect sensor is continuous, and the measured voltage overflows every  $180^\circ$  [3], so it would be very important to ensure the magnet was initially oriented at a value that would encompass both the maximum and minimum joint limit for each actuated universal joint axis. The Bourns PDB08 was selected as the potentiometer due to its small size and internally threaded shaft, which would allow a captive bolt to be inserted as the spider shaft [4]. As a voltage divider at +5 V, the PDB08 would have a resolution of approximately  $40^\circ \text{ V}^{-1}$ . With the 12-bit resolution of the onboard analog to digital converter for myRIO analog inputs, this gives a theoretical resolution of  $\approx 0.048^\circ$ . The potentiometer sliding noise (max. 100 mV) will reduce this during actuated universal joint motion, however this can be partially mitigated with filtering.

### C. Preventing String Failure

One reoccurring issue with the original experiments were the twisted string actuator strings breaking at high values of  $\theta_s$ , which became more common after a number of twisting and untwisting cycles. Occasionally this was caused by the mechanism operating beyond expected limits for  $\theta_s$  and  $f$  due to a failure of limit monitoring within the control system, but failure would also occur within normal operating conditions.

Analysis of the design and the location of the string failures identified “pinch points” and “bite points”, as shown in figure ??, which could potentially damage the string under high tension, causing it to thin out and lose integrity. By removing these points, by rounding off sharp edges and using an alternative method to secure the string, tying it into a loop instead of using grub screws, eliminated these potential sources of string damage. However, nylon monofilament, as was used for the twisted string actuator string, is still susceptible to torsion fatigue [5], [6] which reduces tensile strength [7]. This means the monofilament string will be increasingly susceptible to failure with more twisting and untwisting cycles. Therefore, the SeaKnight BLADE 0.2mm nylon monofilament was exchanged for 0.2mm Dyneema<sup>®</sup> polyfilament string, as used in [8]. Changes to the design of the string clamp allowed for easier installation of string filament, making polyfilament string a practical option.

### D. Enabling ATA

Active transmission adjustment (ATA) allows the dynamic properties of the actuated universal joint to change during operation, with a trade off between  $f_{\max}$  and  $\dot{p}_{\max}$ . With active transmission adjustment a robot could increase joint force when necessary, such as when lifting a heavy payload, and then return to a faster and more responsive configuration when the payload has been released. As  $r$  has been reduced from 0.013 to 0.0725 as shown in table ??, this reduces the twisted string

actuator stroke range  $p$  for a given actuated universal joint angle range. Now the stroke range is smaller, it can be shifted along the curve of the function in equation ?? without exceeding  $l_{\min}$ . This is done by simply increasing or decreasing  $f_{\min}$ . As shown in figure ??, this changes the range of values of  $f_{\max}$  and  $\dot{p}_{\max}$ . Namely,  $f_{\max}$  decreases and  $\dot{p}_{\max}$  increases as  $f_{\min}$  increases, which changes the transmission properties of the system.

## III. EXPERIMENTAL RESULTS

### A. AUJ Angle Tracking

#### B. Demonstration of the Effects of ATA

As can be seen in figure ??, the effect of increasing  $f_{\min}$  is to decrease  $f_{\max}$  and increase  $\dot{p}_{\max}$ . This has two measurable effects, an increase in total energy consumption for a given follower mass and actuated universal joint angle trajectory, and an increase in the maximum stroke speed for a given  $\theta_{\max}$  for each motor. Therefore to demonstrate the effects of active transmission adjustment, two experiments are conducted. The first measures the total energy consumption for a given actuated universal joint angle trajectory at increasing values of  $f_{\min}$ . The total energy consumption can then be calculated using

$$\Sigma_j = \int_{t_0}^{t_n} \sum_{i=1}^3 v_s a_i(t) |d_i(t)| dt, \quad (1)$$

where  $v_s$  is the motor supply voltage, and  $a_i$  and  $d_i$  are the current consumption and duty cycle  $\in [-1, 1]$  ( $d_i$  has a negative duty cycle when the motor is running in reverse) of motor  $i$  at time  $t$ . Figure ?? shows this increase. The second measures the ability of the actuated universal joint to track a trajectory at a constantly increasing velocity given a constrained  $\theta_{\max}$ . Since increasing  $f_{\min}$  increases  $\dot{p}_{\max}$ , a larger value of  $f_{\min}$  should allow the actuated universal joint to track the trajectory for a longer period of time before falling behind. Figure ?? shows this effect.

Test.

An experiment was also conducted to assess the performance of the system when  $f_{\min}$  is changed while the actuated universal joint is in motion at a non-zero position. The results of this experiment are shown in figure ??, and show minimal disturbance to the actuated universal joint trajectory during the transition.

### C. The Effect of Follower Mass on AUJ Angle Tracking

Figure ?? shows the setpoint and response trajectory for each experiment for both version 1 and version 2. Initially,  $k_p$  was set to the same value as in table ??, however the system was unable to reach a steady state in any configuration other than “No Mass”. Reducing  $k_p$  to 1000 in the weighted configurations solved the steady state issue and resulted in an average maximum tracking error of  $0^\circ$  over all configurations with added mass, similar to the result from the initial experiments. However, for the “No Mass” configuration,  $k_p = 1000$  resulted in a very poor tracking response, whereas  $k_p$  from table ??

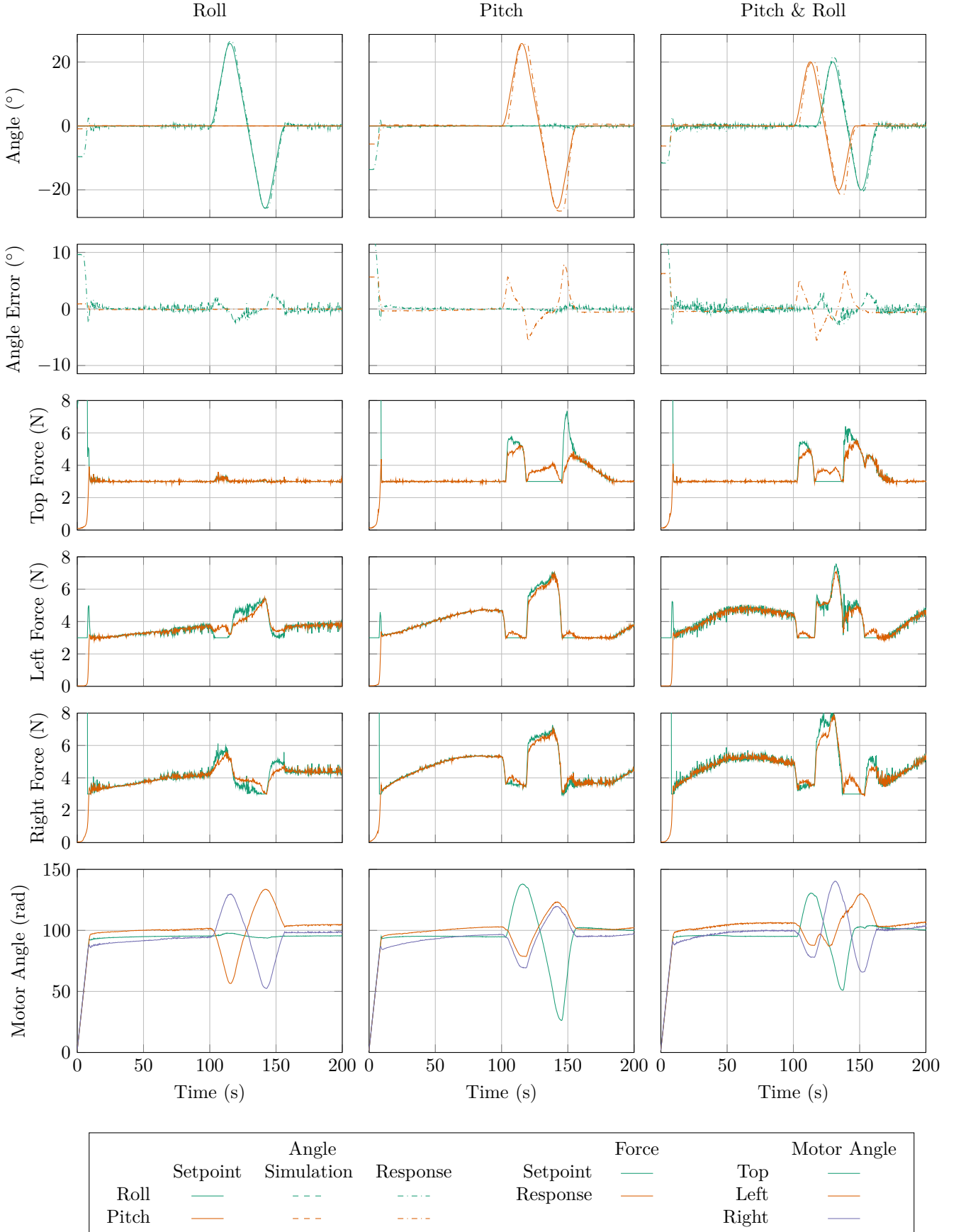
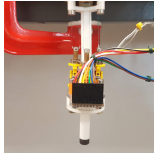
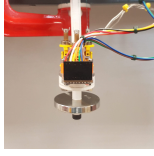

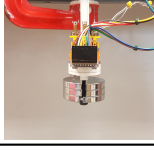


Fig. 1: Plots of the response for three different trajectories, one on only the roll axis  $\theta_1$  (column 1), one on only the pitch axis  $\theta_2$  (column 2), and one on both axes  $\theta_1$  and  $\theta_2$  (column 3). Plots include actuated universal joint orientation, forces at the top, left and right twisted string actuator, and the motor positions. Note the simulation error is very small, so the plot cannot be seen on the graph.

TABLE I: Table of all the follower mass configurations, with the parameters for follower mass  $m$  and follower center of mass  $z$  offset  $\rho_3$ .

Configuration	$m$ [g]	$\rho_3$ [mm]	$I$ [kg m <sup>-2</sup> ]	Image
No Mass	62	3.1	diag ( $2.8 \times 10^{-5}$ , $2.6 \times 10^{-5}$ , $5.2 \times 10^{-6}$ )	
+100 g	160	35	diag ( $1.5 \times 10^{-4}$ , $1.5 \times 10^{-4}$ , $3.7 \times 10^{-5}$ )	
+200 g	260	43	diag ( $1.9 \times 10^{-4}$ , $1.9 \times 10^{-4}$ , $6.9 \times 10^{-5}$ )	
+300 g	360	46	diag ( $2.3 \times 10^{-4}$ , $2.2 \times 10^{-4}$ , $1.0 \times 10^{-4}$ )	

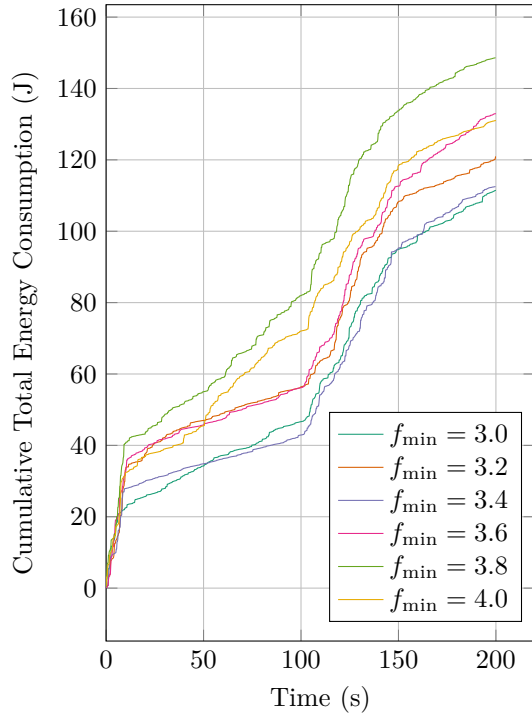


Fig. 2

resulted in a maximum tracking error of  $0^\circ$ , once again similar to the result from the initial experiments. In future implementations gain scheduling can be employed to select the most optimal  $k_p$  for a given follower mass, that allows for the smallest tracking error while being able to reach a

steady state.

#### IV. DISCUSSION

#### V. CONCLUSION

#### VI. ACKNOWLEDGEMENT

This work was supported by a UKRI EPSRC Doctoral Training Partnership [1957210], and by the UKRI Strength in Place Fund [84646 (AMPI)]. The lead author also wishes to thank Dr. Dmitriy Makhnovskiy for his assistance in preliminary research for this publication.

#### REFERENCES

- [1] D. Crosby, J. Carrasco, W. Heath, and A. Weightman, "A novel triad twisted string actuator for controlling a two degrees of freedom joint: Design and experimental validation," in *2022 International Conference on Robotics and Automation (ICRA)*, IEEE, 2022, pp. 11 388–11 394.
- [2] *Bno080 data sheet*, 1.3, Hillcrest Laboratories, Inc., Oct. 2017.
- [3] K. Bienczyk, "Angle measurement using a miniature hall effect position sensor," in *2009 2nd International Students Conference on Electrodynamical and Mechatronics*, IEEE, 2009, pp. 21–22.
- [4] *Pdb08 - 8 mm micro rotary potentiometer*, Bourns, Mar. 2021.
- [5] B. Goswami and J. Hearle, "A comparative study of nylon fiber fracture," *Textile Research Journal*, vol. 46, no. 1, pp. 55–70, 1976.

- [6] M. Toney and P. Schwartz, "Bending and torsional fatigue of nylon 66 monofilaments," *Journal of applied polymer science*, vol. 46, no. 11, pp. 2023–2032, 1992.
- [7] D. Hennessey, E. Carey, C. Simms, A. Hanly, and D. Winter, "Torsion of monofilament and polyfilament sutures under tension decreases suture strength and increases risk of suture fracture," *Journal of the Mechanical Behavior of Biomedical Materials*, vol. 12, pp. 168–173, 2012.
- [8] G. Palli, C. Natale, C. May, C. Melchiorri, and T. Wurtz, "Modeling and control of the twisted string actuation system," *IEEE/ASME Transactions on Mechatronics*, vol. 18, no. 2, pp. 664–673, 2012.



**Dr. Damian J. Crosby** is a Post Doctoral Research Associate in the Department of Mechanical, Aerospace and Civil Engineering, University of Manchester, U.K. He received a B.Sc. in Special Effects Development from The University of Bolton, U.K., in 2010, and a M.Res. in Robotics from The University of Plymouth, U.K., in 2012. He worked as a Research Technician in robotic laser welding at The University of Manchester from 2013 to 2017, and then completed his PhD at the

same university in 2023, developing a robotic tail for improved robot balance when carrying a payload. He has worked on robotic research in the fields of nuclear energy and advanced manufacturing.



**Dr. Joaquin Carrasco** is a Lecturer at the Department of Electrical and Electronic Engineering, University of Manchester, UK. He was born in Abarn, Spain, in 1978. He received the B.Sc. degree in physics and the Ph.D. degree in control engineering from the University of Murcia, Murcia, Spain, in 2004 and 2009, respectively. From 2009 to 2010, he was with the Institute of Measurement and Automatic Control, Leibniz Universitt Hannover, Hannover, Germany. From 2010 to 2011, he was a Research Associate at the Control Systems Centre, School of Electrical and Electronic Engineering, University of Manchester, UK.



**Prof. William P. Heath** is Chair of Feedback and Control in the Department of Electrical and Electronic Engineering, University of Manchester, U.K. He received the B.A. and M.A. degrees in mathematics from Cambridge University, U.K., in 1987 and 1991, and the M.Sc. and Ph.D. degrees in systems and control from the University of Manchester Institute of Science and Technology, U.K., in 1989 and 1992, respectively. He was with Lucas Automotive from 1995 to 1998 and was a Research Academic at the University of Newcastle, Australia from 1998 to 2004. His research interests include absolute stability, multiplier theory, constrained control, and system identification.



**Prof. Andrew Weightman** graduated in 2006 with a PhD in Mechanical Engineering from the University of Leeds. Whilst at the University of Leeds he developed rehabilitation robotic technology for improving upper limb function in adults and children with neurological impairment which was successfully utilised in homes, schools and clinical settings. In 2013 he moved to the University of Manchester, Department of Mechanical, Aerospace and Civil Engineering as a Lecturer in Medical Mechatronics. Prof. Weightman has research interests in biomimetic mobile robotics, rehabilitation robotics, robotics for nuclear decommissioning and collaborative robotics.